

Angiogenesis, Metastasis, and the Cellular Microenvironment**EphB4 Promotes Site-Specific Metastatic Tumor Cell Dissemination by Interacting with Endothelial Cell-Expressed EphrinB2**Mélanie Héroult^{1,2}, Florence Schaffner⁴, Dennis Pfaff^{1,2}, Claudia Prahst^{1,2}, Robert Kirmse³, Simone Kutschera^{1,2}, Maria Riedel¹, Thomas Ludwig³, Peter Vajkoczy⁶, Ralph Graeser⁵, and Hellmut G. Augustin^{1,2}**Abstract**

The tyrosine kinase receptor EphB4 interacts with its ephrinB2 ligand to act as a bidirectional signaling system that mediates adhesion, migration, and guidance by controlling attractive and repulsive activities. Recent findings have shown that hematopoietic cells expressing EphB4 exert adhesive functions towards endothelial cells expressing ephrinB2. We therefore hypothesized that EphB4/ephrinB2 interactions may be involved in the preferential adhesion of EphB4-expressing tumor cells to ephrinB2-expressing endothelial cells. Screening of a panel of human tumor cell lines identified EphB4 expression in nearly all analyzed tumor cell lines. Human A375 melanoma cells engineered to express either full-length EphB4 or truncated EphB4 variants which lack the cytoplasmic catalytic domain (Δ C-EphB4) adhered preferentially to ephrinB2-expressing endothelial cells. Force spectroscopy by atomic force microscopy confirmed, on the single cell level, the rapid and direct adhesive interaction between EphB4 and ephrinB2. Tumor cell trafficking experiments *in vivo* using sensitive luciferase detection techniques revealed significantly more EphB4-expressing A375 cells but not Δ C-EphB4-expressing or mock-transduced control cells in the lungs, the liver, and the kidneys. Correspondingly, ephrinB2 expression was detected in the microvessels of these organs. The specificity of the EphB4-mediated tumor homing phenotype was validated by blocking the EphB4/ephrinB2 interaction with soluble EphB4-Fc. Taken together, these experiments identify adhesive EphB4/ephrinB2 interactions between tumor cells and endothelial cells as a mechanism for the site-specific metastatic dissemination of tumor cells. *Mol Cancer Res*; 8(10); 1297–309. ©2010 AACR.

Introduction

The British pathologist, Stephen Paget, observed as early as 1889 that the distribution pattern of many metastatic tumors does not follow a random pattern that can be explained by trapping of metastasizing tumor cells in a distant blood or lymphatic vessel bed (1). Instead, many tumors seem to “home” preferentially to certain organs. These observations led Paget to develop the “seed-and-soil theory” of tumor spread and metastasis (1, 2). According to this theory, the metastasizing tumor cell (the “seed”) needs

to fall onto fertile “soil” in order to grow. Pioneering animal experiments in the 1970s provided experimental evidence for Paget's theory by establishing the various subclones of the B16 melanoma as a model to study the mechanisms of site-specific metastasis (3, 4). Chemokines (5), endothelial cell adhesion molecules (6, 7), and organ-selectively expressed growth factors (8, 9) have subsequently been implicated in controlling site-specific metastasis. Comparative transcriptomic analyses of primary tumors and metastases have contributed to the definition of gene signatures associated with the metastatic phenotype,

Authors' Affiliations: ¹Vascular Biology and Tumor Angiogenesis, Medical Faculty Mannheim (CBTM), Heidelberg University; ²Vascular Oncology and Metastasis, German Cancer Research Center Heidelberg (DKFZ-ZMBH Alliance); ³Department of Microenvironment of Tumor Cell Invasion, BioQuant-Zentrum, German Cancer Research Center Heidelberg (DKFZ), Heidelberg, Germany; ⁴Department of Vascular Biology and Angiogenesis Research, Tumor Biology Center; ⁵ProQinase GmbH, Freiburg, Germany; and ⁶Department of Neurosurgery, Charite Universitätsmedizin, Berlin, Germany

Note: Supplementary data for this article are available at Molecular Cancer Research Online (<http://mcr.aacrjournals.org/>).

M. Héroult and F. Schaffner contributed equally to this study.

Current address of M. Héroult: Bayer Schering Pharma Research Center, Wuppertal, Germany.

Current address of F. Schaffner: Scripps Research Institute, La Jolla, CA.

Current address of D. Pfaff: Basel University Hospital, Basel, Switzerland.

Current address of C. Prahst: INSERM U833, Paris, France.

Current address of R. Kirmse: University of Colorado at Boulder, Boulder, CO.

Current address of T. Ludwig: Danone Research Wageningen, the Netherlands.

Corresponding Author: Hellmut G. Augustin, Joint Research Division Vascular Biology, Medical Faculty Mannheim (CBTM), Heidelberg University and German Cancer Research Center (DKFZ), Heidelberg, Im Neuenheimer Feld 581, D-69120 Heidelberg, Germany. Phone: 49-6221-42-1500; Fax: 49-6221-42-1515. E-mail: augustin@angiogenese.de

doi: 10.1158/1541-7786.MCR-09-0453

©2010 American Association for Cancer Research.

including signatures of preferential metastasis to specific organs such as the lungs (10-12). Yet, the molecular mechanisms behind Paget's seed-and-soil theory remain largely unresolved to this day.

EphB tyrosine kinase receptors and their transmembrane ephrinB ligands have been identified as a bidirectional signaling system that transduces guidance cues on outgrowing axons and sprouting endothelial cells (13-15). As such, EphB/ephrinB interactions contribute to network formation in the neuronal system as well as in the vascular system. The receptor EphB4 is widely expressed by human tumor cell lines (16, 17). Correspondingly, a strong correlation between EphB4 expression and increased invasiveness has been reported for breast, colon, bladder, prostate, and endometrial tumors as well as for mesothelioma (17-20). Manipulatory experiments have shown the protumorigenic functions of tumor cell-expressed EphB4 in different tumor models (17, 18, 21). A protumorigenic role of EphB4 could be inferred from its stimulating effects on tumor angiogenesis by activating ephrinB2 reverse signaling (22, 23). In contrast, recent reports also suggest the role of EphB4 as a tumor suppressor gene in experimental colorectal tumors, which seems to be supported by expression profiling data in human colorectal tumors (24). Similarly, increased EphB4 phosphorylation inhibits tumorigenicity in mammary tumors (16). These findings suggest that the protumorigenic and antitumorigenic effects of EphB4 expressed by tumor cells are dependent on the cellular context and the microenvironment.

Corresponding to the protumorigenic and antitumorigenic functions of EphB4/ephrinB2 interactions in different tumors (see ref. 25 for recent review), the interaction of EphB4 with its ligand ephrinB2 mediates repulsive as well as attractive functions on neuronal and on vascular cells in a context-dependent manner (13, 14). Work by our and other laboratories has established that endothelial cell ephrinB2 expression and reverse signaling activation is associated with the invasive angiogenic endothelial phenotype suggesting that endothelial-expressed ephrinB2 may be capable of exerting attractive functions (26, 27). We have also shown that selected resting endothelial cell populations express ephrinB2 on their luminal surface and that circulating leukocytes express EphB receptors (28). These findings have shown that bidirectional signaling-dependent EphB4/ephrinB2 interactions control monocyte adhesion to and transmigration through endothelial cells (29). Correspondingly, EphB4 plays a pivotal role in the recruitment of monocytes to ephrinB2-positive endothelial cells to sites of ischemic arteriogenic vascular remodeling (30). EphB receptor-mediated adhesion to endothelial cells has also been observed in other hematopoietic cell types including T cells and dendritic cells (31). Because EphB4/ephrinB2 interactions act as a versatile adhesion-mediating cell-cell interaction and communication system, it was tempting to hypothesize that EphB4 presented by tumor cells might be involved in the site-specific metastatic dissemination of these cells to ephrinB2-positive vascular beds. To study this hypothesis, we established a versatile experimental plat-

form for the sensitive tracing of small numbers of tumor cells in the body. The experiments establish the EphB4/ephrinB2 axis as a mediator of site-specific metastatic tumor cell dissemination.

Materials and Methods

Cells, antibodies, growth factors, and reagents

Human umbilical vein endothelial cells (HUVEC) were purchased from Promocell. A375 melanoma cells (CRL-1619) were obtained from American Type Culture Collection (LGC Standards). FCS was purchased from Biocrom and PAA. Endothelial cell growth medium was from Promocell. Recombinant mouse ephrinB2-Fc, recombinant mouse EphB4-Fc, goat anti-murine ephrinB2 antibody, and goat anti-murine EphB4 antibody were obtained from R&D Systems. Antiphosphotyrosine antibody (sc-7020) was purchased from Santa Cruz Biotechnology, Inc. Human and goat IgG (Fc control) were purchased from Jackson ImmunoResearch.

Plasmid generation and transduction of A375 melanoma cells and HUVEC

EphB4 transduced cells were generated using the pLib IRES luciferase-neomycin vector. The human EphB4-eGFP and the Δ C-EphB4-eGFP (cytoplasmic deletion of amino acids 1-608) fusion proteins were generated by fusion of eGFP to the COOH-terminal sequence of the full-length EphB4 cDNA and the truncated EphB4, respectively (kindly provided by Dr. Daniel Feger, ProQinase, Freiburg, Germany). Human ephrinB2 was subcloned from pcDNA3 into the pLib IRES eGFP-neomycin vector. Human Δ C-ephrinB2 (cytoplasmic deleted corresponding to the last 67 amino acids) was cloned from full-length ephrinB2 and subcloned into the pLib IRES eGFP-neomycin vector. Stable A375 cell lines were generated by retroviral transduction. Briefly, a pantropic packaging cell line (HEK Ampho 293) was transfected with pLib IRES luciferase-neomycin (A375 mock), pLib EphB4-eGFP IRES luciferase-neomycin (A375 EphB4), or pLib Δ C-EphB4-eGFP IRES luciferase-neomycin (A375 Δ C-EphB4) along with 10 μ g of pVSGV (Clontech). The supernatant-containing viruses were collected and A375 cells were infected and selected with G418 (1 mg/mL). The same procedure was used to generate ephrinB2-transduced HUVEC.

RT-PCR

Total cellular RNA was isolated from MDA-MB 231, MDA-MB 468, R30C, HT 29, H 460, A549, PC 3, A375, KLE, ECC-1, HeLa, MIAPACA, Kaposi, LLC, RENCA, lung, and heart endothelial cells using the RNeasy kit (Qiagen) according to the instructions of the manufacturer. RT-PCR was done as previously described (32).

Western blot analysis

A375 transduced cells were left unstimulated or stimulated with ephrinB2-Fc (1 μ g/mL) for 1 hour. Cell lysates were run on a 10% SDS-PAGE gel. Proteins were blotted

onto a polyvinylidene difluoride membrane, blocked with a 3% bovine serum albumin solution, and probed with a monoclonal mouse anti-phosphorylated tyrosine antibody followed by a rabbit anti-mouse horseradish peroxidase. Protein bands were visualized by enhanced chemiluminescence (GE Healthcare). For detection of EphB4 proteins, the membrane was stripped and EphB4 was probed with a goat anti-mouse EphB4 and detected with a rabbit anti-goat horseradish peroxidase. The proteins were visualized using enhanced chemiluminescence.

Luciferase assay

Luciferase activity in cell lysates was measured as follows: cells were counted and lysed in 1× reporter lysis buffer (Promega). The lysates were centrifuged and 10 μL of supernatant was assayed with 40 μL of luciferase assay buffer in a luminometer. The same procedure was applied to measure the luciferase activity in organ lysates. Organs [inguinal lymph nodes (left and right), liver, spleen, intestine, colon, kidney, skeletal muscle, femur, and tibia from the lower left leg, lung, heart, and brain] were harvested in 2 mL of 1× reporter lysis buffer and homogenized using a glass potter. Lysates were centrifuged and 30 μL of the cleared lysate was assayed with 60 μL of luciferase assay buffer using a reader plate luminometer.

Flow cytometry analysis

A375 transduced cells were either left unstimulated or stimulated with ephrinB2-Fc (1 μg/mL) for 1 hour. The cells were detached from culture dishes with HBSS-EDTA, spun down and incubated with 10% goat serum on ice. After washing with HBSS, the unstimulated cells were incubated with ephrinB2-Fc on ice for 15 minutes. All cells were washed and a biotinylated goat anti-human Fc (Caltag, Invitrogen) was added on ice for 25 minutes. The cells were washed and incubated with streptavidin cytochrome conjugate on ice in the dark for 25 minutes. Finally, the cells were washed and fixed with 1% paraformaldehyde. Flow cytometry analysis was done on a Becton Dickinson FACSCalibur. Data from 10,000 cells per sample were analyzed with the CellQuest Cell Cycle Analysis.

Adhesion assay

A375 were labeled using PKH-26 according to the protocols of the manufacturer (Sigma). Labeled cells (50,000 cells) were allowed to adhere to the HUVEC monolayer under agitation for 30 minutes. Thereafter, the medium was removed, the monolayer was carefully washed twice with PBS and the cells were fixed with 4% PFA. Adherent A375 cells from three wells (five fields per well) were quantified using Olympus image analysis software.

Adhesion experiments under flow

Transduced HUVEC were seeded in gelatin-coated flow chamber μ-Slides I (ibidi GmbH) and grown to confluence for flow experiments. HUVECs were pretreated for 1 hour with either human IgG-Fc (1 μg/mL) or EphB4-Fc (1 μg/mL). A375 cells were labeled with PKH-26 accord-

ing to the protocols of the manufacturer (Sigma). Subsequently, 2×10^5 transduced A375 cells/mL were passed over the monolayers with a shear rate of 50 per second for 30 minutes. Nonadherent cells were washed off with PBS and the adherent cells were fixed with 4% PFA for 10 minutes. Adherent A375 cells were quantified in five fields per slide using Olympus image analysis software.

Cellular scratch assay

A monolayer of A375 cells was scratched with a tip and wound closure was monitored over 24 hours. The area at the beginning and at the end of the experiment was measured using the imaging software DP-Soft (Olympus).

Transmigration assay

A375 cells (50,000 cells) were seeded on top of a Transwell coated with gelatin (5 μm pore) and allowed to migrate towards FCS (used as chemoattractant in the bottom chamber) for 4 hours. Cells on the filter were fixed with 4% PFA and stained with Hoechst. Nonmigrated cells were removed from the top of the filter with a cotton swab. Migrated cells on the bottom of the filter were quantified in four fields per filter using Olympus image analysis software.

Single cell force spectroscopy by atomic force microscopy

Cantilevers (CSC 12 from Ultrasharp, μMash) were cleaned in 1% Hellmanex (Hellma) for 1 hour and rinsed with ultrapure water prior to incubation for 15 minutes in acetone. Cantilevers were then rinsed with ultrapure water and incubated in 40 μL of 50 μg/mL fibronectin in PBS and incubated for 1 hour in a humidified chamber at room temperature. Cantilevers were rinsed with PBS and mounted onto the cantilever holder directly prior to use. The basic principles of single cell force spectroscopy have been described elsewhere in detail (33, 34). In brief, single cell force spectroscopy was done with a CellHesion Module in combination with a NanoWizard II AFM (JPK Instruments) mounted on an inverted microscope (Axiovert 250 Zeiss). Coverslips of ephrinB2-transduced HUVEC were mounted into the chamber of the BioCell (JPK Instruments) of the atomic force microscopy (AFM) and kept at 37°C in HUVEC medium. Sensitivity and spring constants of each fibronectin-coated cantilever were determined with the build in routines of the NanoWizard II AFM software. Spring constants were in a range of 0.03 and 0.05 N/m. A375 EphB4, ΔC-EphB4, and mock cells were injected in the BioCell and individual cells were attached to the cantilever by utilizing the build in cell capture routine of the AFM software (5 s at 800 pN; Fig. 4B). After capture, cantilever-bound cells were incubated for 5 minutes before positioning them above a single HUVEC. After bringing the cantilever-bound cell into contact with the surface of a single HUVEC, the cells were loaded with a constant force of 800 pN (Fig. 4A). Cells were allowed to interact for time intervals of up to 120 seconds before pulling them apart ("adhesion time"). Subsequently,

a standard adhesion time of 60 seconds was used for all measurements. The delay between individual, successive force-distance measurements was 120 seconds. EphB4-Fc or control human Fc were used to block ephrinB2 expressed by HUVEC. EphB4-Fc or control human Fc (10 $\mu\text{g}/\text{mL}$) were injected into the BioCell and cells were incubated with the polypeptide for 5 minutes before performing force measurements. Individual force-distance curves were analyzed with the software supplied with the AFM and the mean value of the maximum detachment force and the work needed for complete removal of the cells were calculated.

Intracardiac injection

Transduced A375 cells were detached with HBSS-EDTA and suspended at 1×10^6 cells/mL in DMEM. Cells were intracardially injected (100 μL) into the left ventricle of the heart of female NMRI^{nu/nu} mice (Harlan Winkelmann) under isoflurane anesthesia.

For *in vivo* blocking experiments, NMRI^{nu/nu} mice were injected i.p. with 20 μg of recombinant mouse EphB4-Fc (R&D Systems) or with 10 μg of human Fc (Jackson ImmunoResearch) 1 hour prior to tumor cell injection.

EphrinB2 immunostaining

EphrinB2 staining on paraffin-embedded tissues was done using the TSA Biotin system (Perkin-Elmer) according to the protocols of the manufacturer. Briefly, blocking reagent was added onto the sections for 30 minutes. The goat anti-murine ephrinB2 antibody in Tris-NaCl-blocking (TNB) buffer was incubated for 1 hour. After three washes with TNT buffer for 5 minutes, the secondary biotin-labeled rabbit anti-goat antibody (Vector) was incubated for 30 minutes in TNB buffer. After washes, streptavidin horseradish peroxidase was incubated on the sections for 30 minutes. Subsequently, the TSA biotin system amplification was added for 10 minutes. After washes, streptavidin horseradish peroxidase was incubated for 30 minutes and the enzymatic activity was detected by incubating with the peroxidase substrate 3,3'-diaminobenzidine. The enzymatic reaction was stopped in water and sections were counterstained with hematoxylin, dehydrated, and mounted in Permount.

Soft agar colony assay

A layer of 0.75% agarose in DMEM was poured in a six-well plate and allowed to solidify at 4°C. The cells were mixed with 0.4% agarose in DMEM preheated at 48°C. Then, the mixture of agarose and cells was poured on the bottom layer and allowed to solidify for 10 minutes at 4°C and put back into the incubator. The number of colonies formed after 13 days was quantified per field.

Primary lung and heart endothelial cell isolation

Freshly excised murine lungs and heart were dissociated in a solution of collagenase (2 mg/mL) and dispase I (0.5 units/mL) for 1 hour at 37°C. Dissociated tissues were filtered through a cell strainer (100 $\mu\text{mol}/\text{L}$) and the drained cell suspension was washed twice in ice-cold

PBS/2.5% FCS. Cells were then incubated with murine immunoglobulins (1 $\mu\text{g}/\text{mL}$) for 30 minutes at 4°C. Cells were washed twice in ice-cold PBS/2.5% FCS and incubated with a mixture of the following antibodies: rat anti-mouse CD31, rat anti-mouse CD105, and biotinylated isolectin B4 (all at 2.5 $\mu\text{g}/\text{mL}$) for 30 minutes at 4°C. Cells were washed twice, resuspended into 200 μL of PBS/2.5% FCS and incubated with a mixture of goat anti-rat-conjugated microbeads (20 μL ; Miltenyi) and streptavidin-conjugated microbeads (20 μL ; Miltenyi) for 30 minutes at 4°C. Meanwhile, a column was loaded on a magnetic separation unit (Miltenyi) and equilibrated with 500 μL of PBS/0.5% FCS. Cells and bead suspensions were loaded onto the column. The column was washed with 500 μL of PBS/0.5% FCS. After removal of the column from the magnet unit, the cells were eluted with PBS/0.5% FCS using the plunger. The eluted cell suspension was processed identically through a new equilibrated column. The cells were plated onto fibronectin-coated plates.

Statistical analyses

Data are presented as the mean \pm SD or as the mean \pm SEM. Differences between experimental groups were analyzed by unpaired Student's *t* test or Mann-Whitney for unpaired groups. AFM data were analyzed by one-way ANOVA followed by multiple pairwise comparisons (Holm-Sidak). *P* < 0.05 was considered as statistically significant.

Results

Generation of luciferase expressing A375 EphB4, A375 ΔC -EphB4, and A375 mock tumor cells

A panel of 13 human tumor cell lines (breast, lung, melanoma, prostate, endometrium, cervix, colon, pancreas, and sarcoma) was analyzed for their EphB receptor and ephrinB2 ligand expression status (Supplementary Table S1). Among the EphB receptors, EphB2 and EphB4 were most consistently detected. Similarly, ephrinB2 was also expressed by almost all analyzed tumor cell lines. The A375 melanoma cell line expressed nearly undetectable levels of endogenous EphB4 and ephrinB2 (Fig. 1C; data not shown) and was consequently selected for subsequent manipulatory experiments. Parental A375 cells were retrovirally transduced to express either full-length EphB4-eGFP IRES luciferase-neomycin fusion protein, (A375 EphB4), truncated EphB4-eGFP lacking the catalytic cytoplasmic domain IRES luciferase-neomycin fusion protein (A375 ΔC -EphB4), or just the luciferase-neomycin fusion protein (A375 mock). Cells were selected for neomycin resistance to generate transduced cells with uniformly high transgene expression. Fluorescence microscopy (Fig. 1A) and fluorescence-activated cell sorting analysis (Fig. 1B) confirmed cell surface expression of both full-length EphB4 as well as ΔC -EphB4, which lacks the catalytic cytoplasmic domain. Stimulation of cells expressing full-length and truncated EphB4 with ephrinB2-Fc led to the internalization of the EphB4/ephrinB2 complex (Fig. 1B). This was associated

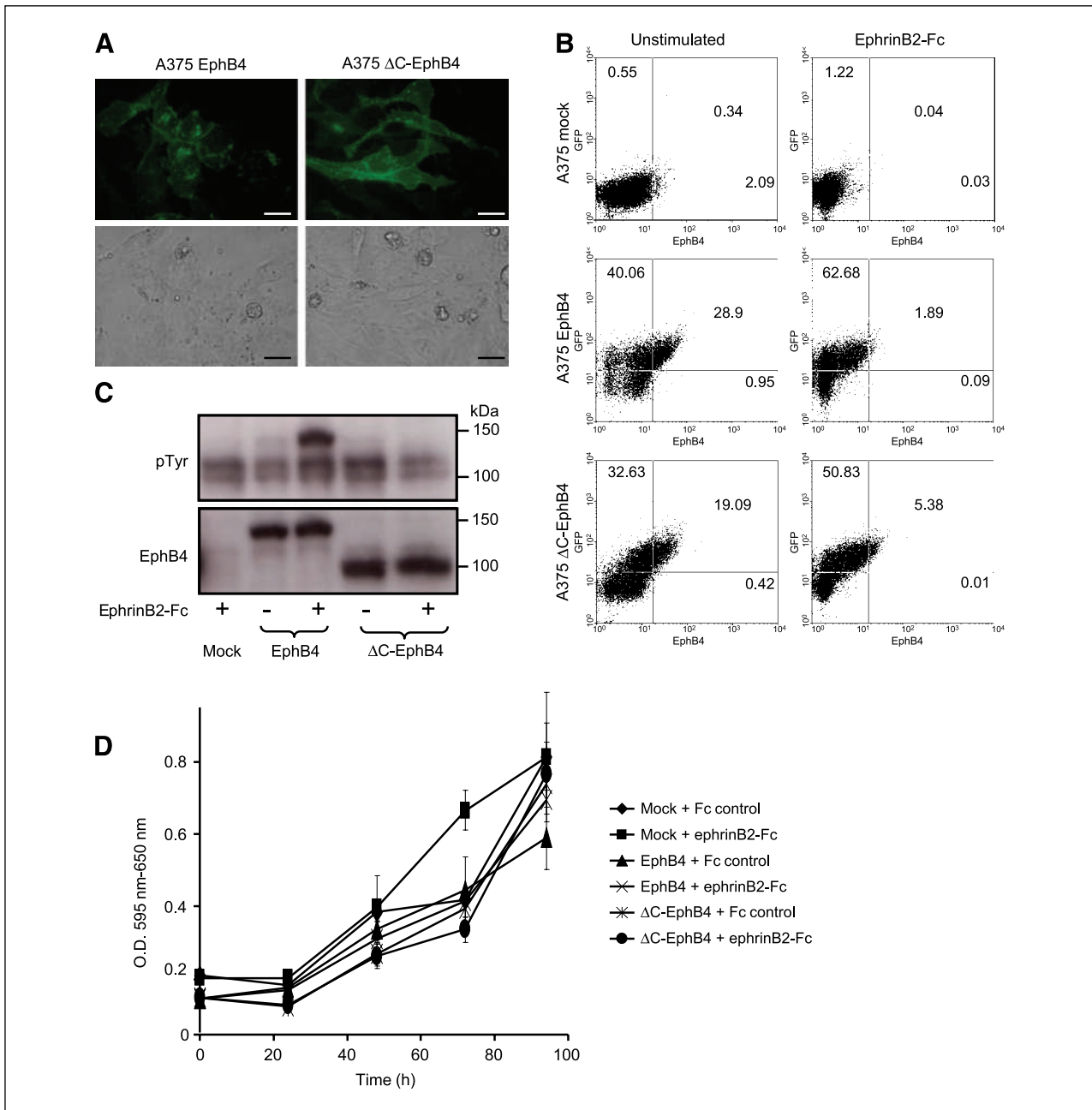


FIGURE 1. EphB4 and Δ C-EphB4 expression in A375 cells. A375 cells were retrovirally transduced to express EphB4-eGFP-IRES-luciferase-neomycin (A375 EphB4), Δ C-EphB4-eGFP-IRES-luciferase-neomycin (A375 Δ C-EphB4), or luciferase-neomycin (A375 mock). A, EphB4-eGFP and Δ C-EphB4-eGFP were detected by fluorescence microscopy (bar, 20 μ m). B, fluorescence-activated cell sorting analysis verified the cell surface expression of EphB4 and Δ C-EphB4 (left). Stimulation of transduced A375 with ephrinB2-Fc for 1 h led to endocytosis of the resulting EphB4/ephrinB2 complex (right). C, A375 EphB4, A375 Δ C-EphB4, or A375 mock were stimulated with ephrinB2-Fc and lysed for Western blot analysis. EphrinB2-Fc induced EphB4 phosphorylation (top, lane 3). The membrane was stripped and blotted with an anti-EphB4 antibody to confirm equal loading (bottom). D, expression of full-length or truncated EphB4 did not alter the proliferation characteristics of A375 cells. Likewise, stimulation with ephrinB2-Fc did not affect the proliferation of mock-transduced or EphB4-expressing A375 cells.

with EphB4 phosphorylation in full-length, but not in cells expressing truncated EphB4 (Fig. 1C). Taken together, these data confirm proper cell surface presentation, activation characteristics, and endocytosis pattern of the engineered cells expressing EphB4 variants.

EphB4 and Δ C-EphB4 expression affects A375 tumor cell migration but not proliferation

EphB4 expression has been associated with a change in invasiveness and proliferation of tumor cells *in vitro* and has been correlated with tumor progression *in vivo*

(17, 18, 22, 32). We did proliferation assays to analyze if the expression of EphB4 or Δ C-EphB4 altered A375 cell proliferation in normal growth medium (control Fc) or upon ligand (ephrinB2-Fc) stimulation. Full-length or truncated EphB4 expression did not alter the proliferative behavior of A375 cells in the absence or presence of ephrinB2 stimulation (Fig. 1D). Likewise, EphB4 or Δ C-EphB4 expression did not affect the cells' ability to establish three-dimensional spheroids or to grow colonies in soft agar (Fig. 2A).

To assess the cells' migratory capacity, we did *in vitro* scratch assays. Monolayers of A375 EphB4, A375 Δ C-EphB4, and A375 mock cells were scratch-wounded and wound closure was monitored after 24 hours. Both full-length EphB4 and truncated EphB4-expressing A375 Δ C-EphB4 cells migrated significantly faster than A375 mock cells (Fig. 2B), suggesting that the extracellular

domain of EphB4 is sufficient for a promigratory phenotype of A375 melanoma cells. Stimulation with clustered recombinant human Fc or ephrinB2-Fc did not change A375 migration, confirming that the promigratory effect of EphB4 is independent of forward signaling (data not shown). Furthermore, we tested the chemotactic properties of transduced A375 cells in a transmigration assay. A375 Δ C-EphB4 and EphB4 cells migrated faster through gelatin-coated filters compared with mock cells (Fig. 2C, black columns). This increased migration was not significantly affected by stimulation with ephrinB2-Fc (Fig. 2C, gray columns) or after seeding the cells on different matrices, e.g., type IV collagen, fibronectin, or Matrigel (Supplementary Fig. S1). Changes in migratory capacity were not associated with changes in the cells' proteolytic activity as confirmed by matrix metalloproteinase-2 and matrix metalloproteinase-9 activities in gelatin-zymograms (Supplementary Fig. S2).

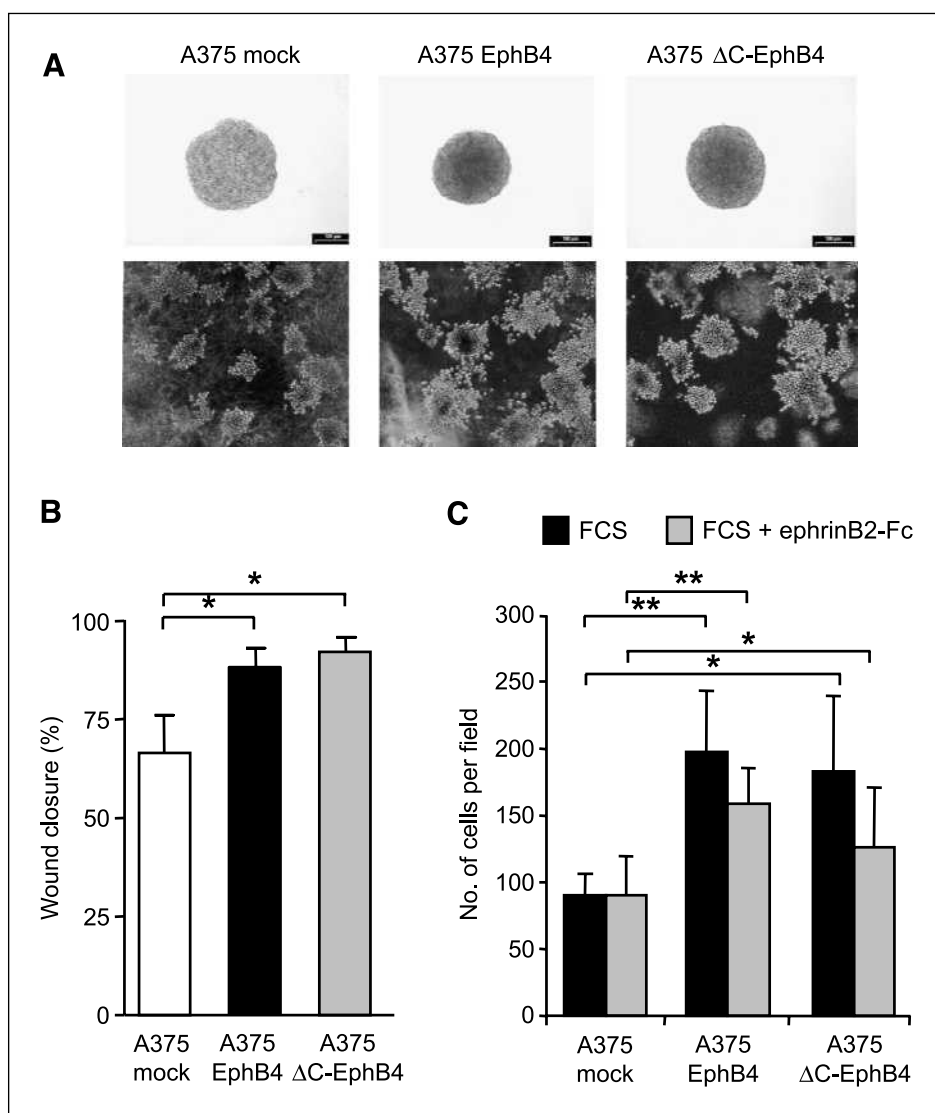


FIGURE 2. Anchorage-independent growth and migration of A375 EphB4, Δ C-EphB4, and mock-transduced A375 cells.

A, A375 EphB4, A375 Δ C-EphB4, and A375 mock cells were able to establish three-dimensional spheroids in a similar manner (top). Likewise, the three cell lines were able to form colonies in soft agar (bottom). Results are expressed as mean \pm SD. Images are representative of at least three independent experiments (bar, 100 μ m). B, A375 cell migration was analyzed in a scratch-wound assay. Wound closure was quantified after 24 h. Both A375 EphB4 (black columns) and Δ C-EphB4 (gray columns) migrated faster than A375 mock cells (open columns) cells. C, transmigration of A375 transduced cells was studied in a modified Boyden chamber assay. A375 cells migrated to the lower side of a gelatin-coated insert in response to FCS (black columns) or to FCS and ephrinB2-Fc (gray columns). The migrated cells were stained with Hoechst and counted in three different fields. A375 EphB4 and A375 Δ C-EphB4 cells transmigrated faster than A375 mock cells in response to FCS. Results are expressed as mean \pm SD of three independent experiments (*, $P < 0.05$; **, $P < 0.005$; bar, 200 μ m).

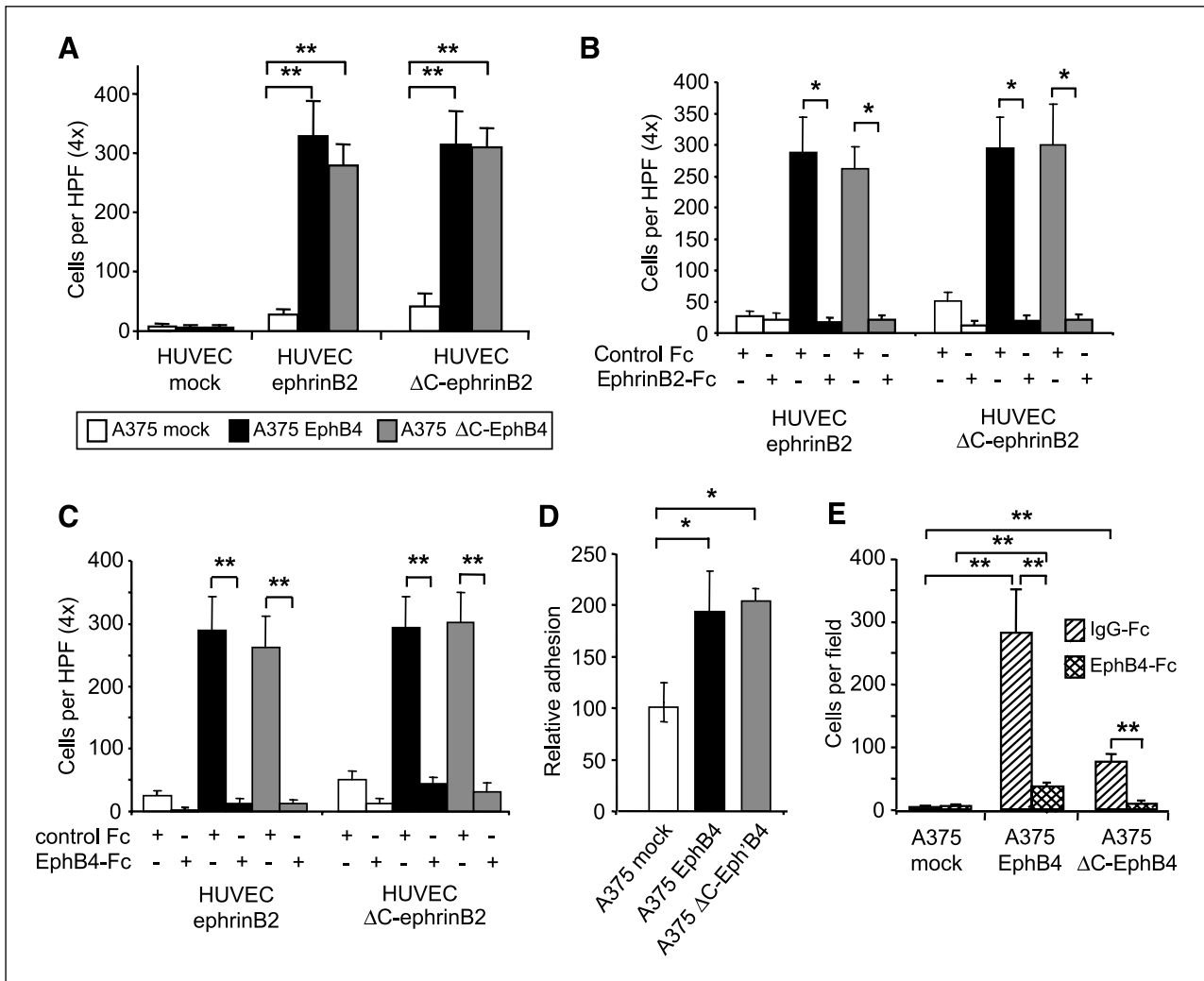


FIGURE 3. Adhesion of A375 EphB4 and A375 ΔC-EphB4 to ephrinB2-coated surfaces or to ephrinB2-expressing endothelial cells. **A**, PKH-labeled A375 EphB4 (black columns), A375 ΔC-EphB4 (gray columns), or A375 mock cells (open columns) were allowed to adhere to HUVEC (ephrinB2, ΔC-ephrinB2, or mock) under gentle agitation for 30 min. A375 EphB4 and ΔC-EphB4 cells preferentially adhered to ephrinB2 and ΔC-ephrinB2 HUVEC. **B**, A375 transduced cells were stimulated with ephrinB2-Fc (1 μg/mL) or control Fc (1 μg/mL) prior to adhesion to HUVEC for 1 h. Preincubation with ephrinB2-Fc inhibited the preferential adhesion of A375 EphB4 and A375 ΔC-EphB4 cells to HUVEC expressing either ephrinB2 or ΔC-ephrinB2. Control Fc did not affect adhesion. **C**, ephrinB2 or ΔC-ephrinB2-expressing HUVEC were stimulated with EphB4-Fc (1 μg/mL) or control Fc (1 μg/mL) prior to A375 cell adhesion for 1 h. Preincubation with EphB4-Fc inhibited the preferential adhesion of A375 EphB4 and A375 ΔC-EphB4 cells to HUVEC expressing either ephrinB2 or ΔC-ephrinB2. Control Fc did not affect adhesion. **D**, A375 EphB4 and A375 ΔC-EphB4 adhered preferentially to ephrinB2-Fc-coated dishes compared with control-Fc-coated dishes whose adhesion was set to 100%. **E**, A375 EphB4, but not A375 ΔC-EphB4 or mock-transfected A375 cells, adhered strongly to ephrinB2-expressing HUVEC under flow. EphB4-Fc (1 μg/mL) blocked EphB4-mediated adhesion to ephrinB2-expressing HUVEC. The graphs show one representative experiment of three independent experiments with similar results (two independent experiments in E). Results are expressed as mean ± SD (*, $P < 0.05$; **, $P < 0.005$).

EphB4 expression exerts a proadhesive phenotype on tumor cells *in vitro*

Bidirectional signaling between EphB4 and ephrinB2 has been reported to transduce both attractive as well as repulsive signals on contacting cells. We consequently tested the ability of EphB4-expressing A375 cells to adhere to ephrinB2-expressing endothelial cells. The number of A375 EphB4 and A375 ΔC-EphB4-expressing cells, which adhered to HUVEC monolayers expressing either full-length ephrinB2 or ΔC-ephrinB2 was significantly in-

creased compared with A375 mock cells (Fig. 3A). As shown in Fig. 1B, ephrinB2-Fc stimulation induced the internalization of cell surface EphB4 or ΔC-EphB4. To assess the specificity of EphB4/ephrinB2-mediated tumor cell adhesion to endothelial cells, tumor cells were preincubated with ephrinB2-Fc prior to allowing them to adhere to HUVEC. EphrinB2-Fc stimulation of the A375 EphB4 variants dramatically reduced the ability of A375 to adhere to ephrinB2 or to ΔC-ephrinB2 expressing HUVEC (Fig. 3B). Correspondingly, we blocked the adhesion of

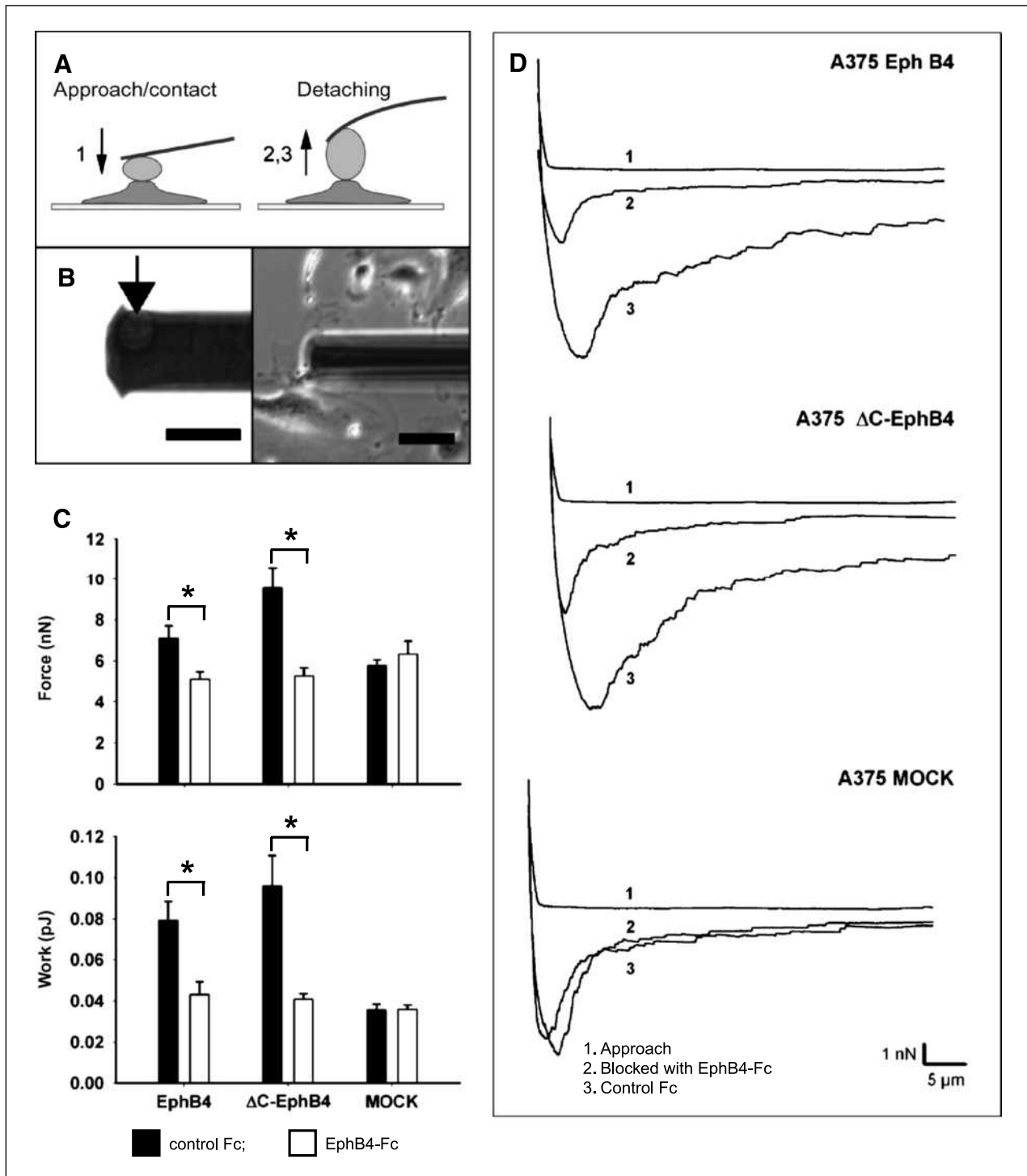


FIGURE 4. Single cell force spectroscopy by AFM. A, schematic model of the force measurements. A single cell was attached to the AFM cantilever and brought in contact with the underlying cell layer (1). After a given adhesion time, the cell was lifted (2, 3) until it detached. B, an individual A375 cell was attached to the cantilever (arrow, left) and localized over a layer of HUVEC (right; columns, 30 μm). C, single cell force spectroscopy data of the interaction between A375 EphB4, A375 ΔC-EphB4, and control transduced cells with HUVEC expressing ephrinB2. The approach and withdrawal speed was set to 10 μm/s. Cell surface contact was maintained for a constant force of 800 pN for 60 s. The average, maximum unbinding force and average unbinding work are displayed for control conditions (black columns) or after the addition of EphB4-Fc (open columns). Each column represents the mean values of 10 to 15 individual force-distance curves. D, representative force-distance curves of individual measurements are shown for A375 cells expressing A375 EphB4 (top), A375 ΔC-EphB4 (center), or A375 mock cells (bottom). (1) Approach of the cantilever-bound cell towards the surface and subsequent contact to the HUVEC. Unbinding force-distance curves of A375 cells in the presence (2) or absence (3) of EphB4-Fc.

A375 EphB4 or Δ C-EphB4 cells to ephrinB2-expressing HUVEC monolayers by treating HUVEC with EphB4-Fc prior to tumor cell adhesion. The different A375 transductants adhered all with similar efficacy to HUVEC ephrinB2 or HUVEC Δ C-ephrinB2 (Fig. 3C), suggesting that ephrinB2 reverse signaling is dispensable for EphB4-mediated tumor cell adhesion to HUVEC. This was also confirmed by using ephrinB2-Fc-coated surface instead of an ephrinB2-expressing endothelial cell monolayer. A375 EphB4 and A375 Δ C-EphB4 but not A375 mock cells adhered specifically to ephrinB2-Fc-coated surfaces (Fig. 3D). Lastly, we did adhesion experiments with the different tumor EphB4 transfectants to ephrinB2-expressing HUVEC under laminar flow. Unlike mock-transfected cells, EphB4-transfected A375 cells strongly adhere to ephrinB2-expressing HUVEC in flow chamber experiments (Fig. 3E). Adhesion of EphB4-expressing cells could be completely blocked by EphB4-Fc (Fig. 3E). Importantly, Δ C-EphB4 cells adhered much more weakly to ephrinB2-expressing HUVEC under flow than full-length EphB4 transfectants indicating that firm adhesion to endothelial cells is EphB4 forward signaling-dependent (Fig. 3E).

To directly quantify the adhesive strength mediated by the interaction between ephrinB2 and EphB4, we did single cell force spectroscopy experiments by AFM. Sin-

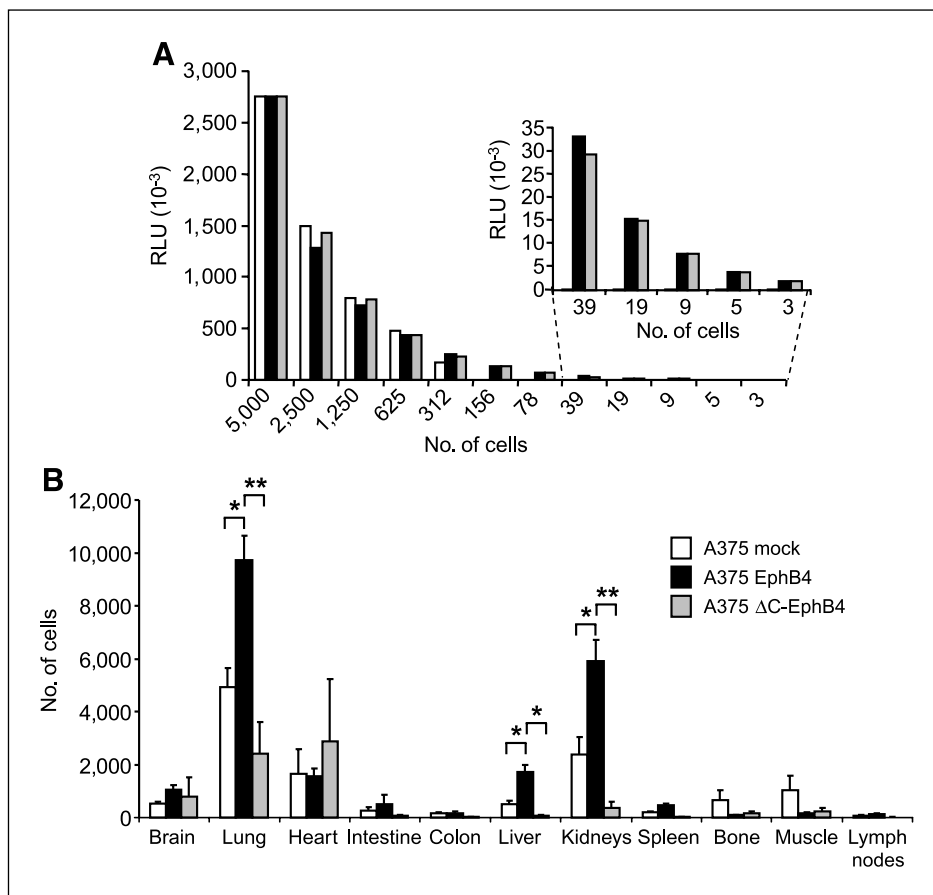
gle, cantilever-bound A375 EphB4, A375 Δ C-EphB4, or A375 mock cells were used to probe HUVEC ephrinB2 (Fig. 4). The maximum unbinding force between A375 cells and HUVEC reached a plateau within 120 seconds of adhesion time (data not shown). Thus, an adhesion time of 60 seconds was used for all subsequent measurements. The average maximum unbinding force and average unbinding work of A375 EphB4 and A375 Δ C-EphB4 cells were significantly higher than observed in A375 mock cells (Fig. 4B and C). Taken together, these experiments show that the extracellular domains of EphB4 and ephrinB2 support strong tumor cell adhesion to endothelial cells.

EphB4 mediates tumor cell adhesion to ephrinB2-expressing endothelium *in vivo*

To translate the *in vitro* observation that EphB4-positive tumor cells adhere to ephrinB2-expressing endothelial cells, we established a sensitive luciferase-based cell tracing technique. This technique allowed the tracing of tumor cells adhering to ephrinB2-positive endothelium *in vivo*. Titration experiments validated the uniformly high luciferase expression levels of the different A375 cell lines and allowed the reliable quantitation of less than 50 tumor cells (Fig. 5A). These titration experiments were also done to

FIGURE 5. Luciferase expression and *in vivo* distribution pattern of A375 EphB4, Δ C-EphB4, and A375 mock-transduced cells.

A, transduced A375 (5,000 cells) were lysed and the luciferase activity was measured in triplicate. The three cell lines expressed comparable levels of luciferase activity. The graph shows one representative measurement of three independent experiments with similar results. B, transduced A375 (100,000 cells) were injected in the left ventricle of the heart. The organs were harvested 1 h after injection, homogenized, and luciferase activity was measured for each organ lysate. The number of A375 expressing EphB4 cells (black columns) was significantly higher in the lungs, liver and kidneys compared with A375 mock (open columns), and A375 Δ C-EphB4-transduced cells (gray columns). The graph shows one representative experiment out of two independent experiments with similar results using six to seven mice per experimental group. Data are expressed as mean \pm SEM (*, $P < 0.05$; **, $P < 0.005$).



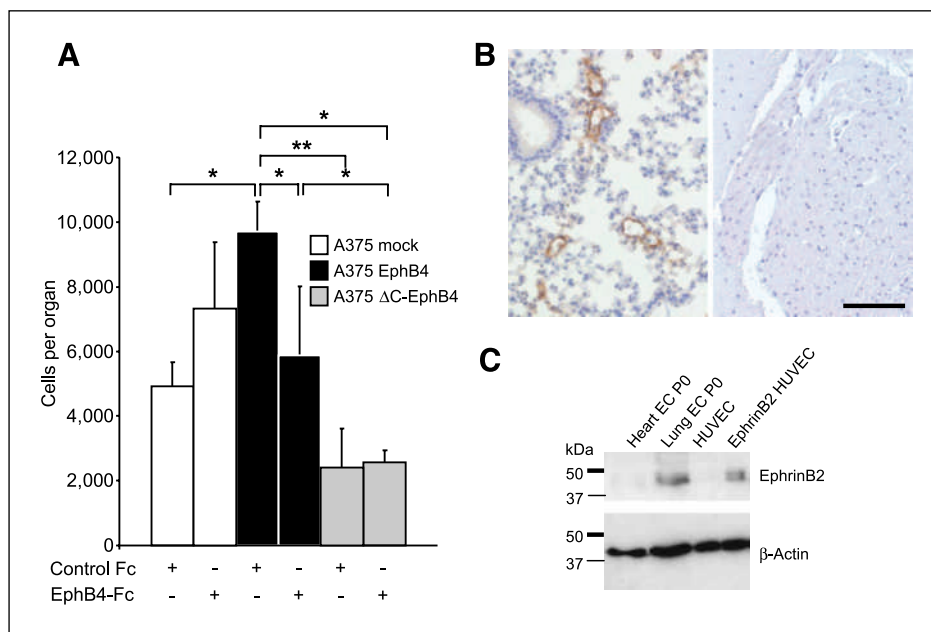


FIGURE 6. Blockade of A375 EphB4 homing to the lungs by soluble EphB4 receptor. **A**, blocking of ephrinB2 by EphB4-Fc or a control human Fc was done by i.p. injection 1 h prior to tumor cell injection. The distribution of the injected tumor cells was analyzed by luciferase activity in organ lysates. Injection of EphB4-Fc blocked the preferential homing of A375 EphB4 cells to the lungs (black columns) but did not affect the trafficking of A375 mock (open columns) and A375 ΔC-EphB4-transduced cells (gray columns). The graph shows one representative experiment out of two experiments with similar results using six to eight mice per experimental group. The data are expressed as mean \pm SEM (*, $P < 0.05$; **, $P < 0.001$). **B**, ephrinB2 was expressed by a subset of microvessels in the lungs (brown staining; hematoxylin counterstain; left), whereas endothelial cells in the heart did not express detectable levels of ephrinB2 (right; bar, 100 μ m). **C**, protein was isolated from primary lung and heart endothelial cells (P0 = freshly isolated, not cultured cells from adult mice). Western blot analysis showed specific expression of ephrinB2 in lung endothelial cells, but not in endothelial cells isolated from the heart. Passaged HUVEC and ephrinB2-expressing HUVEC served as negative and positive controls for ephrinB2 expression, respectively.

scale the system in order to translate later luciferase measurements into absolute cell numbers.

Luciferase-expressing tumor cells were injected into the arterial blood flow. Mice were sacrificed 1 hour after arterial injection of the A375 EphB4, A375 ΔC-EphB4, and A375 mock cells. The 1-hour time point was selected on the basis of preliminary experiments revealing that cell distribution within the first minutes predominantly reflected relative tissue perfusion and not specific homing. The inguinal lymph nodes, lungs, heart, liver, spleen, intestine, colon, kidneys, muscle, brain, and the left femur (bone) were harvested and homogenized, and luciferase activity was measured in each of these organs. The highest luciferase activities were measured in the most vascularized organs (i.e., lungs, liver, kidneys, brain, and heart; Fig. 5B). However, significantly more A375 EphB4 cells were detected in the lungs, the liver, and the kidneys compared with A375 mock and A375 ΔC-EphB4 (Fig. 5B).

To assess the specificity of the observed EphB4-mediated tumor cell homing phenotype, we did an independent series of experiments to examine if recombinant EphB4-Fc could block preferential trafficking of A375 EphB4 cells to the lungs. I.p. injection of EphB4-Fc 1 hour prior to tumor cell injection completely blocked the homing of A375 EphB4 cells to the lungs (Fig. 6A), suggesting that soluble EphB4-Fc either inhibited adhesion or that it induced endocytosis of endothelial cell ephrinB2.

Preferential homing of A375 EphB4 cells and EphB4-Fc blocking strongly suggested a direct interaction of injected cells with endothelial cell-expressed ephrinB2. We confirmed endothelial cell ephrinB2 expression in the lungs where it was expressed by a subset of microvessels (Fig. 6B). Expression was mostly confined to small arteries and arterioles that were covered by α SMA-positive mural cells (Supplementary Fig. S3). EphrinB2 expression was also observed in kidney glomerular capillary endothelial cells as well as a subset of kidney arteriolar α SMA-positive and α SMA-negative microvessels (Supplementary Fig. S3). To more directly validate organ-specific differences in endothelial cell ephrinB2 expression, we isolated endothelial cells from mouse lung and heart and compared ephrinB2 protein expression. The lung and the heart were used for these experiments because A375 EphB4 cells preferentially home to the lung (see Fig. 5B). Despite the strong vascularization of the heart, ephrinB2 protein was detected in endothelial cells isolated from lungs, but not in endothelial cells isolated from heart (Fig. 6C).

Discussion

Originally considered as the ultimate hallmark of cellular anarchy resulting from random survival of cells released from the primary tumor (35), tumor progression and metastasis are now recognized as a result of the selective

growth of specialized subpopulations of highly metastatic cells endowed with specific properties that enable them to complete each step of the metastatic process (2, 36). A metastatic tumor cell must be capable of breaking away from the primary tumor, to induce angiogenesis, to invade lymphatic or blood vessels, to intravasate into the lumen of an invaded vessel, to survive the rigid biophysical forces of the circulation, to lodge and to adhere in the vasculature of a distant organ, to extravasate the vessel, to survive at a distant site, and it must eventually be capable of initiating growth at the secondary site which again includes the requirement of inducing angiogenesis. Each of these steps of the metastatic cascade is considered rate-limiting for the process, making metastasis in fact a very inefficient biological process which is only accomplished by the large number of tumor cells that can be shed into the circulation from a primary tumor. Importantly, although a primary tumor may be capable of shedding large numbers of tumor cells, most of these may undergo apoptotic cell death and only few may have metastasis-initiating capacity (cancer stem cells? refs. 37, 38). Likewise, metastatic dissemination of tumor cells may be a necessary albeit not sufficient requirement for the growth of tumor cells at distant sites because tumor dormancy mechanisms may be limiting for the formation of metastasis following metastatic dissemination (39).

A critical step of the metastatic cascade is the lodging of systemically disseminating tumor cells at distant sites. Circulating tumor cells get trapped in the next capillary bed that they encounter. Yet, they may leave their primary site of lodging again if they are not retained by specific adhesive interactions to endothelial cells which is the first interface of a metastasizing tumor cell in a distant organ. In the present study, we have addressed the specific hypothesis that tumor cells which express EphB4 may be involved in the metastatic homing to ephrinB2-expressing vascular beds. This was an attractive hypothesis given that most human tumors express EphB4 (17-20) and that distinct endothelial cell populations express ephrinB2 on their luminal aspect (28). Likewise, it has recently been reported that tumor cell-expressed EphB4 promotes metastatic dissemination (40). Combining cellular experiments with sensitive luciferase-based *in vivo* cell trafficking assays, we show in the present study that (a) the extracellular domain of EphB4 expressed by tumor cells and the extracellular domain of ephrinB2 expressed by endothelial cells is sufficient to mediate rapid and stable adhesion between tumor cells and endothelial cells, (b) the extracellular domain of EphB4 is sufficient to mediate enhanced tumor cell migration, (c) full-length tumor cell expressed EphB4, but not signaling incompetent cytoplasmically truncated Δ C-EphB4 is capable of mediating preferential trafficking of tumor cells to the lungs, the liver, and the kidneys, but not to the similarly well-perfused heart, (d) lung endothelial cells, but not heart endothelial cells, express ephrinB2, and (e) the preferential EphB4-mediated trafficking of EphB4-expressing tumor cells can be blocked by treatment with soluble EphB4-Fc given prior to tumor cell

injection. The experiments shed novel light into the mechanisms of systemic tumor cell dissemination and identify a potentially important molecular mechanism of site-specific metastasis.

The experimental design of the study was deliberately aimed at concentrating mechanistically on a single step of the metastatic cascade rather than performing spontaneous metastases experiments originating from orthotopically growing primary tumors. Tumor cell lodging and subsequent adhesion to endothelial cells may be one of the most rate-limiting steps of the metastatic cascade (41, 42). Different mechanisms have previously been implicated in the adhesion of tumor cells to endothelial cells including the involvement of E-selectin and P-selectin, the binding to coagulation factors like fibrin or tissue factor as well as a contribution of platelets (43-46). Likewise, several lung endothelial cell-expressed molecules have been implicated in lung-specific metastasis. These include dipeptidyl peptidase IV (6), the Ca^{2+} -sensitive chloride channel protein 1 (also called Lu-ECAM-1; ref. 47), and metacadherin (48). These studies illustrate the remarkable heterogeneity of endothelial cells in different vascular beds which provide a vascular address code for the site-specific distribution of metastasizing tumor cells analogous to the homing of circulating leukocytes (49).

This study deliberately focused on the early steps of systemic tumor cell dissemination to trace the fate of tumor cells that were directly injected into the systemic arterial circulation. An arterial injection approach was applied to avoid the first-pass lung effect following the widely practiced tail vein injection technique. The preferential homing phenotype of EphB4-expressing tumor cells was rapidly detectable and analyzed 1 hour after tumor cell injection. Yet, this phenotype was sustained allowing the detection of living, luciferase-expressing tumor cells in the lungs even weeks after injection (data not shown), suggesting that injected tumor cells in fact establish dormant micrometastases at distant sites. This dormancy phenotype is in distinct contrast to the observation that the A375 melanoma cells used form rapidly growing highly angiogenic tumors when grafted subcutaneously. The observation that lung metastatic tumor cell dissemination might lead to dormant microtumors is also compatible with the concept that a distinct set of genes may confer organ site-selective metastagenicity potential, whereas a different set of genes might contribute to metastatic virulence allowing the growth of originally dormant microtumors at the secondary site (10-12).

Only full-length EphB4 expressing, but not signaling, incompetent Δ C-EphB4 A375 cells exhibited a preferential homing phenotype to ephrinB2-positive vascular beds *in vivo* suggesting that forward EphB4 tyrosine kinase signaling was involved in this process. This corresponded to the finding of the cellular flow chamber experiments in which only full-length EphB4 transfected cells, but not signaling-incompetent Δ C-EphB4 A375 cells, adhered to ephrinB2 expressing HUVEC. Yet, in static cellular models, the extracellular domains of EphB4 and ephrinB2 were

sufficient to mediate rapid adhesion between the corresponding receptor- and ligand-expressing tumor and endothelial cells. Likewise, Δ C-EphB4-expressing A375 cells exhibited a signaling-independent promigratory phenotype. These findings support the concept that EphB receptors might be able to support cellular functions in a kinase-dependent and kinase-independent manner. For example, the catalytic activity of EphB3 is required for the inhibition of integrin-mediated adhesion of colorectal tumor cells. In turn, a kinase-independent signaling pathway involving Rho GTPases is operative in full-length and kinase-deficient EphB3 receptor-expressing cells mediating inhibition of directional cell migration (50). Kinase-independent Eph receptor functions have been reported in other experimental systems as well. A genetic study of VAB-1, a single Eph orthologue in *C. elegans*, revealed severe neuronal and epithelial defects upon targeting of the receptor, but only a mild phenotype upon deletion of the cytoplasmic catalytic domain (51). Similarly, several downstream signaling pathways including RhoGTPases might link EphB receptor function to melanoma cell migration and invasion (52, 53). Along these lines, the results of this study show for the first time that EphB4 confers a promigratory and a proadhesive phenotype to tumor cells independent of its kinase domain. Yet, the full-length signaling competent receptor is required to mediate the EphB4-dependent site-specific metastatic tumor cell dissemination phenotype.

References

1. Paget S. The distribution of secondary growths in cancer of the breast. *Lancet* 1889;1:571–3.
2. Fidler IJ. The pathogenesis of cancer metastasis: the 'seed and soil' hypothesis revisited. *Nat Rev Cancer* 2003;3:453–8.
3. Fidler IJ, Kripke ML. Metastasis results from preexisting variant cells within a malignant tumor. *Science* 1977;197:893–5.
4. Hart IR, Fidler IJ. Role of organ selectivity in the determination of metastatic patterns of B16 melanoma. *Cancer Res* 1980;40:2281–7.
5. Muller A, Homey B, Soto H, et al. Involvement of chemokine receptors in breast cancer metastasis. *Nature* 2001;410:50–6.
6. Johnson RC, Zhu D, Augustin-Voss HG, Pauli BU. Lung endothelial dipeptidyl peptidase IV is an adhesion molecule for lung-metastatic rat breast and prostate carcinoma cells. *J Cell Biol* 1993;121:1423–32.
7. Pauli BU, Augustin-Voss HG, el-Sabban ME, Johnson RC, Hammer DA. Organ-preference of metastasis. The role of endothelial cell adhesion molecules. *Cancer Metastasis Rev* 1990;9:175–89.
8. Rossi MC, Zetter BR. Selective stimulation of prostatic carcinoma cell proliferation by transferrin. *Proc Natl Acad Sci U S A* 1992;89:6197–201.
9. Menter DG, Herrmann JL, Nicolson GL. The role of trophic factors and autocrine/paracrine growth factors in brain metastasis. *Clin Exp Metastasis* 1995;13:67–88.
10. Minn AJ, Kang Y, Serganova I, et al. Distinct organ-specific metastatic potential of individual breast cancer cells and primary tumors. *J Clin Invest* 2005;115:44–55.
11. Minn AJ, Gupta GP, Siegel PM, et al. Genes that mediate breast cancer metastasis to lung. *Nature* 2005;436:518–24.
12. Landemaine T, Jackson A, Bellahcene A, et al. A six-gene signature predicting breast cancer lung metastasis. *Cancer Res* 2008;68:6092–9.
13. Klein R. Eph/ephrin signaling in morphogenesis, neural development and plasticity. *Curr Opin Cell Biol* 2004;16:580–9.
14. Adams RH, Alitalo K. Molecular regulation of angiogenesis and lymphangiogenesis. *Nat Rev Mol Cell Biol* 2007;8:464–78.
15. Poliakov A, Cotrina M, Wilkinson DG. Diverse roles of eph receptors and ephrins in the regulation of cell migration and tissue assembly. *Dev Cell* 2004;7:465–80.
16. Noren NK, Foos G, Hauser CA, Pasquale EB. The EphB4 receptor suppresses breast cancer cell tumorigenicity through an Abl-Crk pathway. *Nat Cell Biol* 2006;8:815–25.
17. Kumar SR, Singh J, Xia G, et al. Receptor tyrosine kinase EphB4 is a survival factor in breast cancer. *Am J Pathol* 2006;169:279–93.
18. Xia G, Kumar SR, Masood R, et al. EphB4 expression and biological significance in prostate cancer. *Cancer Res* 2005;65:4623–32.
19. Takai N, Miyazaki T, Fujisawa K, Nasu K, Miyakawa I. Expression of receptor tyrosine kinase EphB4 and its ligand ephrin-B2 is associated with malignant potential in endometrial cancer. *Oncol Rep* 2001;8:567–73.
20. Xia G, Kumar SR, Stein JP, et al. EphB4 receptor tyrosine kinase is expressed in bladder cancer and provides signals for cell survival. *Oncogene* 2006;25:769–80.
21. Masood R, Kumar SR, Sinha UK, et al. EphB4 provides survival advantage to squamous cell carcinoma of the head and neck. *Int J Cancer* 2006;119:1236–48.
22. Noren NK, Lu M, Freeman AL, Koolpe M, Pasquale EB. Interplay between EphB4 on tumor cells and vascular ephrin-B2 regulates tumor growth. *Proc Natl Acad Sci U S A* 2004;101:5583–8.
23. Kertesz N, Krasnoperov V, Reddy R, et al. The soluble extracellular domain of EphB4 (sEphB4) antagonizes EphB4-2 interaction, modulates angiogenesis, and inhibits tumor growth. *Blood* 2006;107:2330–8.
24. Battle E, Bacani J, Begthel H, et al. EphB receptor activity suppresses colorectal cancer progression. *Nature* 2005;435:1126–30.

Disclosure of Potential Conflicts of Interest

No potential conflicts of interest were disclosed.

Grant Support

Deutsche Forschungsgemeinschaft within the priority grant SPP1190 "The tumor-vessel interface" (Au83/9-3). H.G. Augustin is supported by an endowed chair from the Aventis Foundation.

The costs of publication of this article were defrayed in part by the payment of page charges. This article must therefore be hereby marked *advertisement* in accordance with 18 U.S.C. Section 1734 solely to indicate this fact.

Received 10/12/2009; revised 08/02/2010; accepted 09/04/2010; published OnlineFirst 09/13/2010.

25. Pasquale EB. Eph receptors and ephrins in cancer: bidirectional signaling and beyond. *Nat Rev Cancer* 2010;10:165–80.
26. Adams RH, Diella F, Hennig S, Helmbacher F, Deutsch U, Klein R. The cytoplasmic domain of the ligand ephrinB2 is required for vascular morphogenesis but not cranial neural crest migration. *Cell* 2001;104:57–69.
27. Fuller T, Korff T, Kilian A, Dandekar G, Augustin HG. Forward EphB4 signaling in endothelial cells controls cellular repulsion and segregation from ephrinB2 positive cells. *J Cell Sci* 2003;116:2461–70.
28. Korff T, Dandekar G, Pfaff D, et al. Endothelial ephrinB2 is controlled by microenvironmental determinants and associates context-dependently with CD31. *Arterioscler Thromb Vasc Biol* 2006;26:468–74.
29. Pfaff D, Heroult M, Riedel M, et al. Involvement of endothelial ephrinB2 in adhesion and transmigration of EphB expressing monocytes. *J Cell Sci* 2008;121:3842–50.
30. Korff T, Braun J, Pfaff D, Augustin HG, Hecker M. Role of ephrinB2 expression in endothelial cells during arteriogenesis: impact on smooth muscle cell migration and monocyte recruitment. *Blood* 2008;112:73–81.
31. Pfaff D, Fiedler U, Augustin HG. Emerging roles of the Angiopoietin-Tie and the ephrin-Eph systems as regulators of cell trafficking. *J Leukoc Biol* 2006;80:719–26.
32. Martiny-Baron G, Korff T, Schaffner F, et al. Inhibition of tumor growth and angiogenesis by soluble EphB4. *Neoplasia* 2004;6:248–57.
33. Ludwig T, Kirmse R, Poole K, Schwarz US. Probing cellular microenvironments and tissue remodeling by atomic force microscopy. *Pflügers Arch* 2008;456:29–49.
34. Franz CM, Taubenberger A, Puech PH, Muller DJ. Studying integrin-mediated cell adhesion at the single-molecule level using AFM force spectroscopy. *Sci STKE* 2007;pl5.
35. Fidler IJ. Host and tumour factors in cancer metastasis. *Eur J Clin Invest* 1990;20:481–6.
36. Gupta GP, Massague J. Cancer metastasis: building a framework. *Cell* 2006;127:679–95.
37. Nguyen DX, Bos PD, Massagué J. Metastasis: from dissemination to organ-specific colonization. *Nat Rev Cancer* 2006;9:274–84.
38. Mimeault M, Batra SK. New promising drug targets in cancer- and metastasis-initiating cells. *Drug Discov Today* 2010;15:354–64.
39. Aguirre-Ghiso JA. Models, mechanisms and clinical evidence for cancer dormancy. *Nat Rev Cancer* 2007;7:834–46.
40. Kumar SR, Schemet JS, Ley EJ, et al. Preferential induction of EphB4 over EphB2 and its implication in colorectal cancer progression. *Cancer Res* 2009;69:3736–45.
41. Steeg PS. Cancer: micromanagement of metastasis. *Nature* 2007;449:671–3.
42. Weil RJ, Palmieri DC, Bronder JL, Stark AM, Steeg PS. Breast cancer metastasis to the central nervous system. *Am J Pathol* 2005;167:913–20.
43. Mannori G, Santoro D, Carter L, Corless C, Nelson RM, Bevilacqua MP. Inhibition of colon carcinoma cell lung colony formation by a soluble form of E-selectin. *Am J Pathol* 1997;151:233–43.
44. Kim YJ, Borsig L, Varki NM, Varki A. P-selectin deficiency attenuates tumor growth and metastasis. *Proc Natl Acad Sci U S A* 1998;95:9325–30.
45. Jain S, Zuka M, Liu J, et al. Platelet glycoprotein Iba supports experimental lung metastasis. *Proc Natl Acad Sci U S A* 2007;104:9024–8.
46. Palumbo JS, Talmage KE, Massari JV, et al. Tumor cell-associated tissue factor and circulating hemostatic factors cooperate to increase metastatic potential through natural killer cell-dependent and-independent mechanisms. *Blood* 2007;110:133–41.
47. Zhu DZ, Cheng CF, Pauli BU. Mediation of lung metastasis of murine melanomas by a lung-specific endothelial cell adhesion molecule. *Proc Natl Acad Sci U S A* 1991;88:9568–72.
48. Brown DM, Ruoslahti E. Metadherin, a cell surface protein in breast tumors that mediates lung metastasis. *Cancer Cell* 2004;5:365–74.
49. Springer TA. Traffic signals for lymphocyte recirculation and leukocyte emigration: the multistep paradigm. *Cell* 1994;76:301–14.
50. Miao H, Strebhardt K, Pasquale EB, Shen TL, Guan JL, Wang B. Inhibition of integrin-mediated cell adhesion but not directional cell migration requires catalytic activity of EphB3 receptor tyrosine kinase. Role of Rho family small GTPases. *J Biol Chem* 2005;280:923–32.
51. George SE, Simokat K, Hardin J, Chisholm AD. The VAB-1 Eph receptor tyrosine kinase functions in neural and epithelial morphogenesis in *C. elegans*. *Cell* 1998;92:633–43.
52. Yang NY, Pasquale EB, Owen LB, Ethell IM. The EphB4 receptor-tyrosine kinase promotes the migration of melanoma cells through Rho-mediated actin cytoskeleton reorganization. *J Biol Chem* 2006;281:32574–86.
53. Sakamoto H, Zhang XQ, Suenobu S, Ohbo K, Ogawa M, Suda T. Cell adhesion to ephrinb2 is induced by EphB4 independently of its kinase activity. *Biochem Biophys Res Commun* 2004;321:681–7.

Molecular Cancer Research

EphB4 Promotes Site-Specific Metastatic Tumor Cell Dissemination by Interacting with Endothelial Cell-Expressed EphrinB2

Mélanie Héroult, Florence Schaffner, Dennis Pfaff, et al.

Mol Cancer Res 2010;8:1297-1309. Published OnlineFirst September 13, 2010.

Updated version Access the most recent version of this article at:
doi:[10.1158/1541-7786.MCR-09-0453](https://doi.org/10.1158/1541-7786.MCR-09-0453)

Supplementary Material Access the most recent supplemental material at:
<http://mcr.aacrjournals.org/content/suppl/2011/10/20/1541-7786.MCR-09-0453.DC1>

Cited articles This article cites 52 articles, 19 of which you can access for free at:
<http://mcr.aacrjournals.org/content/8/10/1297.full#ref-list-1>

Citing articles This article has been cited by 1 HighWire-hosted articles. Access the articles at:
<http://mcr.aacrjournals.org/content/8/10/1297.full#related-urls>

E-mail alerts [Sign up to receive free email-alerts](#) related to this article or journal.

Reprints and Subscriptions To order reprints of this article or to subscribe to the journal, contact the AACR Publications Department at pubs@aacr.org.

Permissions To request permission to re-use all or part of this article, use this link
<http://mcr.aacrjournals.org/content/8/10/1297>.
Click on "Request Permissions" which will take you to the Copyright Clearance Center's (CCC) Rightslink site.